Ring-shaped D-band E-plane filtering coupler

Chen, Xun; Wang, Yi; Zhang, Qingfeng

DOI:
10.1109/LMWC.2021.3082524

Document Version
Peer reviewed version

Citation for published version (Harvard):
Chen, X, Wang, Y & Zhang, Q 2021, 'Ring-shaped D-band E-plane filtering coupler', *IEEE Microwave and Wireless Components Letters*, vol. 31, no. 8, 9438618, pp. 953-956.
https://doi.org/10.1109/LMWC.2021.3082524

Ring-Shaped D-band E-Plane Filtering Coupler

Xun Chen, *Student Member IEEE*, Yi Wang, *Senior Member IEEE* and Qingfeng Zhang, *Senior Member IEEE*

***Abstract*—This paper presents a ring-shaped E-plane filtering coupler working at 150 GHz with a high performance. The coupler is based on cavity resonators. Unlike the conventional ones, the four resonators in this coupler are all bent along their length direction and connected end to end, forming a closed circle. By adjusting the radius of the circle, three of the resonators work on TE_{101} mode while the other is on TE_{102} mode. The coupler can be split through E-plane and the measured response of the coupler has an excellent agreement with the simulation, with a low amplitude imbalance of 0.31 dB, insertion loss of 0.12 - 0.46 dB, and over 20-dB return loss and isolation.**

***Index Terms*—filtering coupler, E-plane, D-band.**

I. Introduction

COUPLERS are important passive components in RF communications, radars and measurement systems. They are used in transceivers [1], [2], manifold multiplexers [3], and Butler matrices [4]-[6]. Two main transmission media are adopted to build couplers. One is waveguide and the other is microstrip line. As the operation frequency becomes higher, for example, at 30 GHz or above, the losses from microstrip lines are increasingly prohibitive for some high-performance requirements. This work targets the increasing popular D-band (110 - 170 GHz), which presents great application potentials in radars and point-to-point links. Couplers working in D-band or above have been reported in [7]-[11], all based on waveguide branch-line structures. Compared with microstrip lines, waveguide offers lower insertion loss especially when splitting and assembling from the favorable plane (e.g., E-plane in the case of TE_{10} rectangular waveguides). At these high millimeter-wave (mm-Wave) frequencies, the additional insertion loss from the interconnection between devices could become dominant. This makes the functional integration between traditionally cascaded components (such as couplers and filters) highly desirable.

Couplers with embedded filtering function but without occupying additional footprint have been reported using four-port coupled resonator structures. Microstrip-line based filtering 180° couplers were shown in [4],[12],[13]. The out-of-phase and isolation ports were achieved by using a combination of inductive and capacitive couplings. Another approach, reported in [6], used resonators working on TE_{101} and TE_{102} mode to realize the opposite coupling. No capacitive coupling iris is needed in this case. This is very desirable as the capacitive iris is usually much narrower than the inductive one. The manufacturability and dimension tolerance would be big problems if the capacitive iris exists in D-band waveguides.

In this letter, an E-plane 180° waveguide coupler working at 150 GHz with integrated filtering function is presented. A combination of TE_{101} and TE_{102} resonators is chosen to realize the opposite signs in coupling. To accommodate the different lengths of the resonators and split the structure in the favorable E-plane, the rectangular resonators have been bent along the length direction and coupled through inductive irises, forming an annular shape. The coupler not only achieves an embedded Chebyshev filtering function, but also removes losses associated with the interconnection from the otherwise separate coupler and filter. The measurement showed high performance and an excellent agreement with the simulation, verifying both the design and the fabrication techniques.

II. Topology and Coupling Matrix

Fig. 1 shows the topology of the filtering coupler, with three TE_{101} mode resonators and one TE_{102} mode resonator. They are

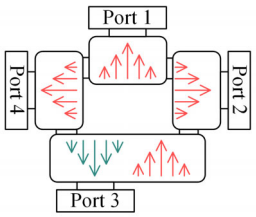

Fig. 1. E-field pattern of the working mode in the schematic diagram of the filtering coupler.

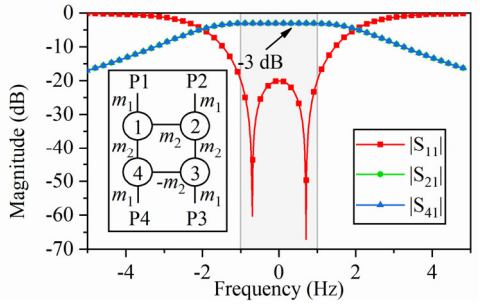

Fig. 2. Theoretical magnitude response from the synthesized coupling matrix.

X. Chen and Q. Zhang are with the Southern University of Science and Technology, Shenzhen 518055, China (e-mail: zhang.qf@sustc.edu.cn).

X. Chen and Y. Wang are with the School of Electrical, Electronic and Computer Engineering, The University of Birmingham, Birmingham B15 2TT, U.K. (e-mail: Y.Wang.1@bham.ac.uk).

The work was supported by the U.K. Engineering and Physical Science Research Council (EPSRC) under Contract EP/S013113/1 and supported in part by the National Natural Science Foundation of China under Grant 61871207 and in part by the Shenzhen Science and Technology Innovation Committee Funds under Grant JCYJ20190809115419425. (Corresponding author: Yi Wang and Qingfeng Zhang.).

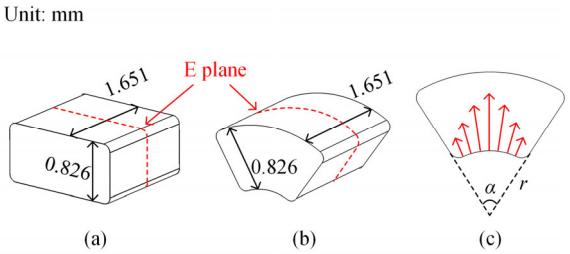

Fig. 3. Rectangular resonator versus fan-shape resonator: (a) original rectangular resonator; (b) fan-shape resonator used in this letter; (c) projected electric field pattern on the E-plane of the dominant resonant mode.

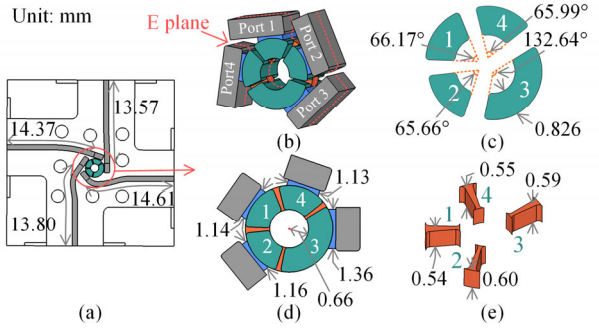

Fig. 4. Dimensions of the filtering coupler. (a) The complete model of the filtering coupler . (b) The overall-view of the filtering coupler. (c) Bending angle of each resonators. (d) Width and height of each port and the widths of the irises to ports. (e) Width of the inter-resonator irises.

all coupled through inductive irises. Different from the H-plane coupler in [6], the coupler is split along the favourable E-plane. The arrows in Fig. 1 indicate the E-field pattern of the standing waves. The TE_{102} mode brings a 180° phase shift, which replaces the use of capacitive coupling. Based on this topology (also shown in the inset of Fig. 2), the coupling matrix can be synthesized. The coupling values are derived from a second-order Chebyshev filter [13]. m_1 = 1.2265 and m_2 = 1.1753. Even higher frequency selectivity may be realized by either introducing transmission zeros or increasing the order of the filter. The theoretical magnitude response of the coupler from the matrix is shown in Fig. 2. Note $|S_{31}|$ is zero (- ∞ in dB) theoretically.

III. Realization of the Filtering Coupler

To make the layout easier, the conventional rectangular resonators are bent along the length direction, making fan-shaped resonators as shown in Fig. 3. Note that all the internal edges perpendicular to the E-plane (as indicated in red dash line) are blended with 0.1 mm radius to meet the fabrication requirement. The height and width of the resonators are kept the same as the standard D-band waveguide, which is 0.826 mm × 1.651 mm. The front view of the bent resonator, in a fan shape, is shown in Fig. 3(c). The electric field pattern of the dominant TE_{101} resonant mode is illustrated in red arrows. α is the bending angle of the fan-shape resonator and r is the inner radius. These two values, instead of the length, are used to specify the size of the resonator and thus the resonant frequency.

The air-model of the filtering coupler is shown in Fig. 4. The four resonators are laid out in an annular shape to form a

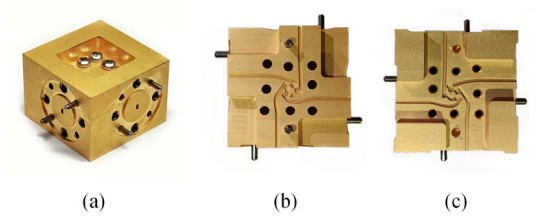

Fig. 5. The fabricated filtering coupler. (a) the overall view. (b) the upper part. (c) the lower part.

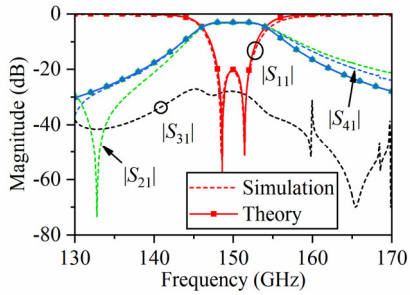

Fig. 6. Simulated response in comparison with the theoretical one from the coupling matrix. Note the theoretical $|S_{31}|$ is - ∞ in dB.

compact footprint. Fig. 4(b) gives the zoomed-in overall-view of the filtering coupler. Its circumference has been divided into eight parts with four resonators (highlighted in green colour) and four coupling irises (in orange) between them. The parts in blue are coupling irises to the ports (in grey colour). All the irises are inductive. Before optimization, the angles of the irises between resonators are all set to be 10°. Three resonators work in TE_{101} mode and the other one in TE_{102} mode. The default bending angle of the TE_{102}-mode resonator is 128° and that of the TE_{101} mode resonators is 64°. The E-plane is depicted using orange dash lines. Note that the irises are also blended for CNC machining as the resonators are.

IV. Fabrication

The coupler was split through the E-plane to minimize the leakage due to the imperfect contact between two split blocks. Four extension waveguide sections are added to facilitate the flange connections and measurement. The fabricated device is shown in Fig. 5. Standard UG387 flanges are used. The coupler structure at the center is surrounded by eight holes for tightening screws. The location and alignment are done by two low-tolerance press-fit pins. The whole block is 27 mm × 27 mm × 20 mm in size. The four ports are uniformly positioned on each side. The dimensions of the coupler are given in Fig. 4. The four resonators are noted with numbers and optimized using CST Microwave Studio~~. The bending angle α of each fan-shaped resonator as well as the radius of the circle determine the resonant frequency~~. Keeping the bending angles unchanged, the resonant frequencies of the two resonators are related to the radius r. The initial sizes of the irises are determined from the coupling matrix by using the well-known dimensioning process for filters [14]. The final optimal radius is shown in Fig. 4(d) to be 0.66 mm. The optimal bending angles are given in Fig. 4(c). The optimized dimensions of the four irises are shown in Fig. 4(e). The heights of the irises control the couplings. The coupler was fabricated using a

high-precision CNC machine with a nominal tolerance of 5 µm. The material is brass and was coated with 2-µm gold.

V. Simulation and Measurement Response

The coupler is designed to work at 150 GHz with 4-GHz bandwidth. In the simulation, the conductivity of gold (4.1×10^7 S/m) was used. The simulated response at Port 1 is shown in Fig. 6, comparing with the theoretical response. The simulated insertion losses of S_{21} and S_{41} are 0.31 dB and 0.26 dB at 150 GHz, respectively. Note there is a transmission zero (TZ) around 133 GHz. Fig. 7 shows the E-field at the TZ when signal is input from Port 1. As can be observed, the E-field is reversed in the area '*a*'. As a result, the signals cancel out in the area '*b*'. This is the reason for the TZ at Port 2.

There are also three weak spikes in the simulated $|S_{31}|$ around 160 GHz, 168 GHz and 170 GHz. Fig. 8 shows the simulated E-field of the coupler at 160 GHz in both contour and arrow forms. It can be noticed that at 160 GHz a TM mode resonates between resonator 3 and Port 3. At 168 GHz, similar TM-mode resonates between resonator 4 and Port 4. At 170 GHz, this happens between resonator 1 and Port 1, resonator 4 and Port 4.

The coupler was connected to two VNA extension modules (N5262AW06), as shown in Fig. 9, for measurement. The other two ports were terminated with loads. The cables connecting to the LO port have a significant influence on the phase response. This influence was minimized by using phase-stable cables and keeping them undisturbed. The measured responses are shown in Fig. 10. The magnitude responses agree extremely well the simulation. Within the operation band, the measured return losses of all four ports are higher than 20 dB. The measured insertion losses of S_{21}, S_{41}, S_{32} and S_{43} are 0.46, 0.15, 0.12 and 0.45 dB, respectively. In terms of phase response, the measurement results also follow the simulations very well. The maximum measured phase imbalance is 5.42° in $\angle S_{23}$ - $\angle S_{43}$. To

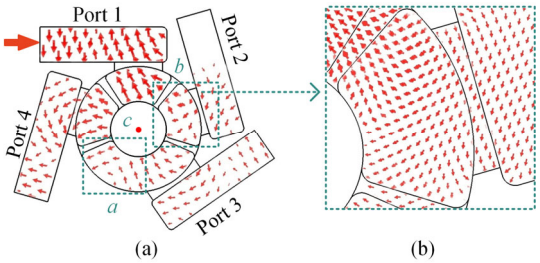

Fig. 7. The E-field of the coupler at the TZ of 132.85 GHz when input from Port 1. (a) E field of the whole coupler. (b) E field in the zoomed-in area '*b*'.

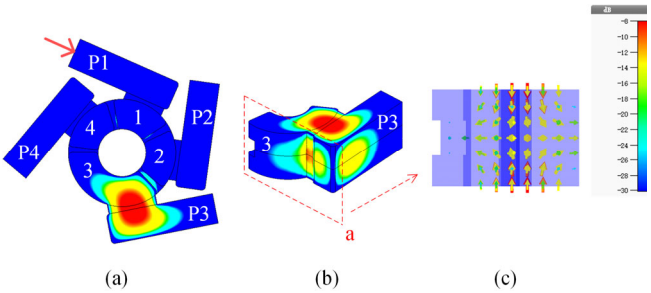

Fig. 8. E-field of the coupler at 160 GHz when input from Port 1: (a) Front view; (b) Perspective view of the selected part. (c) E-field projected to the plane 'a'.

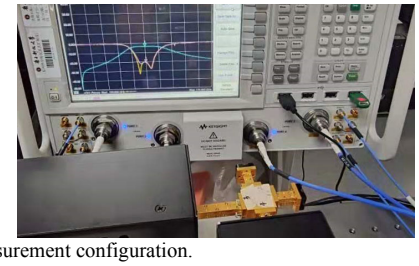

Fig. 9. Measurement configuration.

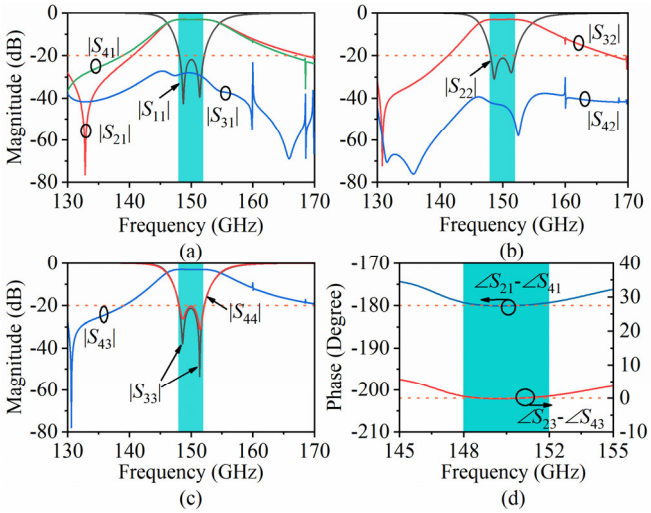

Fig. 10. Simulated and measured responses of the filtering coupler. (a) $|S_{11}|$, $|S_{21}|$, $|S_{31}|$ and $|S_{41}|$. (b) $|S_{22}|$, $|S_{32}|$ and $|S_{42}|$. (c) $|S_{33}|$, $|S_{43}|$, $|S_{44}|$. (d) Phase imbalance.

TABLE I
Comparison with other non-filtering couplers at around D-band

Ref.	RL (dB)	IL (dB)	Iso. (dB)	ΔA (dB)	ΔP (Degree)	CF (GHz)
[7]	10-23	1	15-23	0.4	2	170
[8]	16	0.23	16	0.15	2.5	187
[9]	17	0.8	17	0.3	4	195
[10]	16	0.25	16	0.2	4	187.5
This work	20	0.46	20	0.31	5.42	150

RL = return loss, IL = insertion loss, Iso. = Isolation, ΔA = amplitude imbalance, ΔP = phase imbalance, CF = Center frequency.

the authors' best knowledge, there is no filtering coupler working above 100 GHz reported in literature. The comparison with non-filtering couplers around D-band is shown in Table I. All other couplers are wideband. Apart from the embedded filtering function, this work shows very competitive performance overall with excellent matching and isolation. Considering the narrowband nature, the insertion loss level is also very acceptable. Due to measurement uncertainty, the phase imbalance is slightly higher than expected.

VI. Conclusion

This letter presents a novel design of an E-plane filtering coupler at 150 GHz. The fan-shaped resonator and annular layout make the coupler not only have the embedded filtering function, which eliminates the losses associated with the connecting junction between otherwise separate filters and couplers, but also result in a compact footprint. The measured response agrees very well with the simulated response with a low insertion loss and excellent matching and isolation. This

demonstrated a high performance for the D-band device. This makes the coupler a capable candidate for further applications in more complex passive signal distribution networks.

REFERENCES

[1] T. Bryllert, V. Drakinskiy, K. B. Cooper and J. Stake, "Integrated 200–240-GHz FMCW radar transceiver module," in *IEEE Trans. Microw. Theory Tech.*, vol. 61, no. 10, pp. 3808-3815, Oct. 2013.

[2] P. J. Sobis, A. Emrich and J. Stake, "A low VSWR 2SB schottky receiver," in *IEEE Trans. THz Sci. Tech.*, vol. 1, no. 2, pp. 403-411, Nov. 2011.

[3] T. Kojima, A. Gonzalez, S. Asayama and Y. Uzawa, "Design and development of a hybrid-coupled waveguide multiplexer for a multiband receiver," in *IEEE Trans. Microw. Theory Tech.*, vol. 7, no. 1, pp. 10-19, Jan. 2017.

[4] Q. Shao, F. Chen, Q. Chu and M. J. Lancaster, "Novel filtering 180° hybrid coupler and its application to 2 x 4 filtering butler matrix," in *IEEE Trans. Microw. Theory Tech.*, vol. 66, no. 7, pp. 3288-3296, July 2018.

[5] K. Wincza, S. Gruszczynski and K. Sachse, "Broadband planar fully integrated 8 x 8 Butler Matrix using coupled-line directional couplers," in *IEEE Trans. Microw. Theory Tech.*, vol. 59, no. 10, pp. 2441-2446, Oct. 2011.

[6] V. Tornielli di Crestvolant, P. Martin Iglesias and M. J. Lancaster, "Advanced butler matrices with integrated bandpass filter functions," in *IEEE Trans. Microw. Theory Tech.*, vol. 63, no. 10, pp. 3433-3444, Oct. 2015.

[7] P. J. Sobis, J. Stake and A. Emrich, "A 170 GHz 45° hybrid for submillimeter wave sideband separating subharmonic mixers," in *IEEE Microw.Wireless Compon. Letters*, vol. 18, no. 10, pp. 680-682, Oct. 2008.

[8] H. Rashid, D. Meledin, V. Desmaris and V. Belitsky, "Novel waveguide 3 dB hybrid with improved amplitude imbalance," in *IEEE Microw.Wireless Compon. Letters*, vol. 24, no. 4, pp. 212-214, April 2014.

[9] Z. Niu *et al*., "A Novel 3-dB waveguide hybrid coupler for terahertz operation," in *IEEE Microw. Wireless Compon. Letters*, vol. 29, no. 4, pp. 273-275, April 2019.

[10] H. Rashid, V. Desmaris, V. Belitsky, M. Ruf, T. Bednorz and A. Henkel, "Design of wideband waveguide hybrid with ultra-low amplitude imbalance," in *IEEE Trans. THz Sci. Tech.*, vol. 6, no. 1, pp. 83-90, Jan. 2016.

[11] Z. Niu et al., "Mode analyzing method for fast design of branch waveguide coupler," in *IEEE Trans. Microw. Theory Tech.*, vol. 67, no. 12, pp. 4733-4740, Dec. 2019.

[12] W.-R. Liu, T.-Y. Huang, C.-F. Chen, T.-M. Shen, and R.-B. Wu, "Design of a 180-degree hybrid with Chebyshev filtering response using coupled resonators," in *IEEE MTT-S Int. Microw. Symp. Dig.,* Jun. 2013, pp. 1–3.

[13] C.-K. Lin and S.-J. Chung, "A compact filtering 180 hybrid," *IEEE Trans. Microw. Theory Tech.*, vol. 59, no. 12, pp. 3030–3036, Dec. 2011.

[14] J. S. Hong and M. J. Lancaster, Microstrip Filter for RF/Microwave Application. New York: Wiley, 2001, ch. 7.